Photovoltaic System Performance Enhancement With Non-Tracking Planar Concentrators: Experimental Results and BDRF Based Modelling

Rob W. Andrews *, Andrew Pollard* and Joshua M. Pearce †
* Department of Mechanical and Materials Engineering
Queen's University, Kingston, Ontario, Canada
†Department of Materials Science and Engineering and the Department of Electrical and Computer Engineering
Michigan Technological University, Houghton, MI, USA

***Abstract*—Non-tracking planar concentrators are a low-cost method of increasing the performance of traditional solar photovoltaic (PV) systems. In this study such an outdoor system has been shown to improve energy yield by 45% for a traditional flat glass module and by 35% for a prismatic glass crystalline silicon module. In addition, this paper presents new methodologies for properly modelling this type of system design and experimental results using a bi-directional reflectance function (BDRF) of non-ideal surfaces rather than traditional geometric optics. This methodology allows for the evaluation and eventual optimization of specular and non-specular reflectors in planar concentration systems.**

***Index Terms*—planar concentrator, low concentration, crystal silicon,optics, BDRF, reflectors, booster mirrors**

I. Introduction

Solar photovoltaic (PV) systems are a rapidly expanding market for the creation of sustainable renewable energy, and will play a large role in the future sustainable energy mix [1], [2]. Currently, commercial and utility scale PV installations are predominately arranged in multiple parallel rows of flat modules, which are aligned towards the mean maximum solar intensity.

Each row of modules must be installed with a setback from the row in front of it, to reduce inter-row shading losses and allow maintenance access. The spacing of these rows is highly dependent on the location of the solar array, land availability, and economic constraints which determine the economic performance of a system. [3] Typically, the row spacing is designed to reduce inter-row shading losses which occur in the early morning and late afternoon, however this arrangement leaves the spaces between rows illuminated during the periods of highest solar resource around solar noon [4].

Previous work has investigated the application of planar reflectors for both solar thermal and photovoltaic applications. Much of the early work on planar concentration focused on the improvement of winter time yields for solar thermal systems [5]–[8], some studies found that the optimal orientation for this at high latitudes was a vertical collector with a horizontal reflector [7]. A large body of literature has also looked at various ray tracing models for estimating the increase in irradiation from a given reflector geometry [7]–[17]. Of these models, some account for diffuse reflectors utilizing a combined view factor and specular reflectance model [10], [12], [13], some analyze a two dimensional specular reflectance model [17], and some include experimental results [6], [9], [17], [18]

Currently, planar reflectors are utilized in district heating solar thermal plants in Sweden and Denmark [4], and have been shown experimentally to increase the thermal energy collection at sites of 60°N latitudes by around 30% [17]. It has been proposed that the introduction of non-specular corrugated booster reflectors may further increase the outputs of these fields by up to 8% [4], and studies have characterized the Bi Directional Reflectance Function (BDRF) of these corrugated materials [11].

There are limited examples of experimental studies which address the specific effects of low-level concentration on PV systems, and recently a study was undertaken to identify these additional loss mechanisms [19]. Unfortunately, though the technical feasibility of these systems has been shown, at the time of publication only one entity as commercialized a comparable system for PV applications [20], and because of assumptions made in the design of the system, specialized parallel modules must be utilized with this system.

In order to investigate the potential implementation of these sytems for conventional low-cost PV modules, this study: 1) develops and validates a model using the concept of the BDRF of non ideal surfaces rather than geometric optics and 2) experimentally investigates the systems in an outdoor test site in Kingston, Ontario. This study investigates the potential increase in energy yield and cell temperatures, and develops new methodologies to accurately model the output of these systems. In addition, the new model integrates previous work that analytically investigated the determination of temperature increases, evaluation of diode loading, and identification of angle of incidence effects [19].

II. Experimental Apparatus

A. Outdoors testing

A 6m X 2.5m planar concentrator was installed at the Open Solar Outdoors Test Field (OSOTF) in the fall of 2011 [21]. Two stacks of landscape crystalline silicon (c-Si) modules were arranged in front of the wide planar reflector, and their actual locations with respect to the reflector are shown in Fig 1. One stack had modules with a prismatic glass front sheet, and

the other stack had traditional
had a length of 1m in the plane
had a length of 2.5m in the s

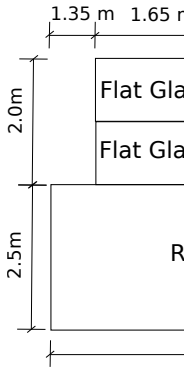

Fig. 1: Schematic of the mode
in the plane normal to the sur

The tilt angles of the s
$90 - \omega = 21°$ and $\gamma - 90$
set of c-Si modules with r

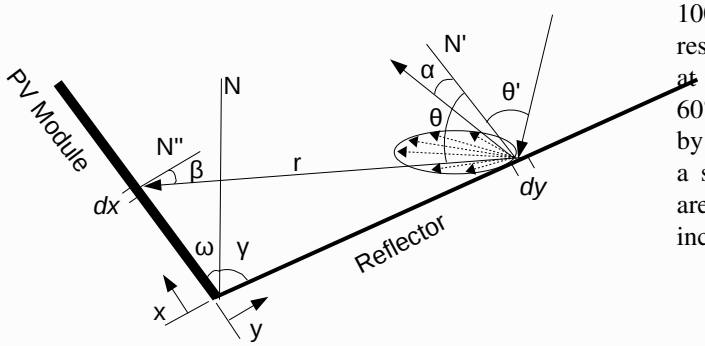

Fig. 2: Plan view of installed system

The concentration system was installed in November 2011, and had two forms of reflector installed: i) semi-diffuse, flexible reflector made of an alumized PET laminate, (Foylon), and used until July, 2012, and ii) a specular aluminzed PET reflector (mylar), which was installed for the remainder of the test period. Both reflectors had a hemispherical reflectivity of approximately 90% on installation, and it is expected that they would degrade optically over time. It should be noted that both these films do not display good long-term weathering characteristics and should not be used for long term testing. However, the reflectivity of these films have shown to be stable for two years of external exposure [22], and have been outside for approximately 1.5 years at the time of publication. The

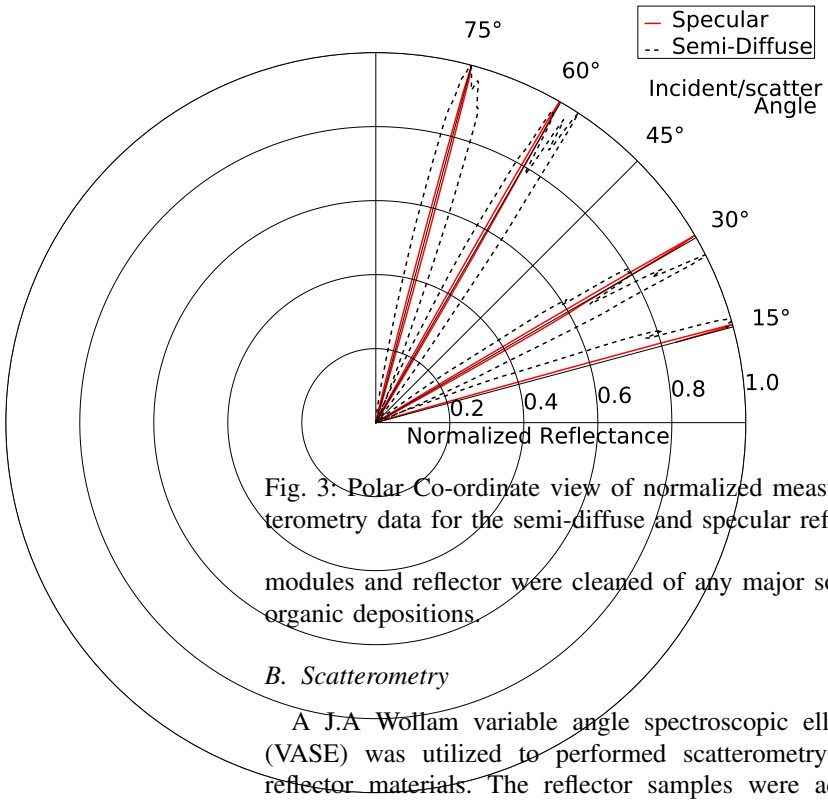

Fig. 3: Polar Co-ordinate view of normalized measured scatterometry data for the semi-diffuse and specular reflector.

modules and reflector were cleaned of any major soiling and organic depositions.

B. Scatterometry

A J.A Wollam variable angle spectroscopic ellipsometer (VASE) was utilized to performed scatterometry on both reflector materials. The reflector samples were adhered to a standard glass slide, which was placed on the rotating sample mount of the VASE. Scattered irradiation was measured using the collimated receiver from angles of -10° to 10° degrees from specular, and at wavelengths of 300nm-1000nm in increments of 100nm. The sample was rotated with respect to the light source, and scatterometry was measured at angles of incidence relative to the reflector surface of 75°, 60°,30°,15°. The reflectivity at each wavelength was weighted by the quantum efficincy of a c-Si module, in order to derive a spectrally responsive reflectivity. The experimental results are shown normalized by the maximum reflectivity at each incidence angle in Fig 3.

III. Modelling

A reflectance model based on a BDRF for an isotropic roughened surface is developed here to predict the performance of the reflector system. The validated model methodology presented in this paper uses the concepts of the BDRF of non-ideal surfaces rather than traditional geometric optics [23], [24]. In addition, this methodology allows for the evaluation of non-specular reflectors in planar concentration systems, which has been shown to increase the energy yields from these systems compared to purely specular reflectors. [4], [25]

The BDRF classifies the three dimensional scattering of light from a surface, and was thoroughly defined in a theoretical framework by Beckman and Spizzichino [26]. Recently, BDRF modelling and research has been a large focus in the fields of computer graphics [23], [27]–[29]. In this paper, a modified version of the Cook-Torrance model is used, which is a commonly used computer graphics model capable of

simulating nearly specular to highly diffuse and anisotropic surfaces [23], [24].

The BDRF defines irradiance reaching a module as a function of both the angle of incidence (θ') and the angle of viewing (θ) of the light. In the case of a perfectly specular reflector, the BDRF resembles the Dirac function, with a value of 1 at θ=θ', and 0 at any other viewing angle, and this is the assumption of a ray-tracing concentrator model. However, real surfaces reflect light in a distribution as defined by the materials BDRF, and is a combination of both diffuse and specular reflections.

A. Model Domain

The domain being considered in this model is shown as a function of the representative angles in Fig 2. An integrative approach is taken in the analysis, where the contribution of irradiation to a differential point on the PV module (dx) from each differential scattering element on the reflector (dy) in the direction of dx (θ) is computed. Thus, in order to determine the irradiation on the surface of the module, an integration is performed along the two principle directions of the array, x and y.

B. Model Derivation

This model is based on a set of simplifying assumptions to decrease computational time and simplify analysis:

1) The reflector is assumed to be infinite and regular along its length. Therefore reflection is only considered in a two dimensional plane normal to the infinite dimension.
2) Because the reflector is infinite, any azimuthal scattering of light is assumed to impact the surface of the modules in the two dimensional plane. The physical interpretation of this is that any light that is scattered azimuthally will eventually impact the module surface, and the two dimensional plane aggregates all the azimuthal scattering from along the infinite length of the reflector.
3) The reflector is a broadband reflector, and spectral attenuation is not taken into account.

Recalling the model domain that is depicted in Fig 2, Equation 1 shows the radiant intensity per unit depth (W/m) that is impacting the plane reflector at point dx. Equation 2 shows the value of reflected radiant intensity per unit depth through a differential angle (W/mθ). Note that the BDRF is normalized such that $\int_0^{\pi} BDRF d\theta = 1$. Equation 3 shows the radiant intensity per unit depth that strikes the surface of the module. Note that θ is defined in Equation 4 in terms of the angle of incidence of the differential ray onto the surface of the module (β) and the distance the ray has travelled (r)

$$E_{i_{plane}} = E_i cos(\theta') dx \quad (1)$$

$$E_{refl} = E_{i_{plane}} BDRF(\theta, \theta') \rho \quad (2)$$

$$E_{module} = E_{refl} d\theta \quad (3)$$

$$d\theta = \frac{dycos(\beta)}{r} \quad (4)$$

Equations 1-4 can be combined and integrated along the characteristic dimensions, and multiplied by the depth of the module being analyzed (D_{module}) and results in Equation 5. Note that the BDRF has been replaced by a 2-D normalized Beckmann distribution.

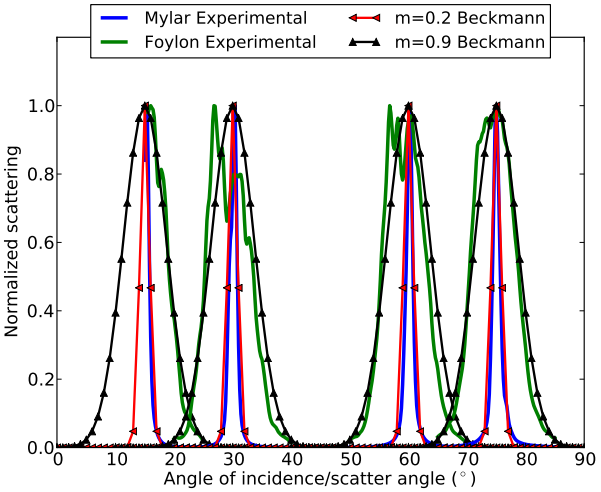

Fig. 4: Comparison of measured scatterometry results from both reflector materials to modelled BDRF distributions for two values of the roughness coefficient (m).

$$Q_o = D_{module} \int_0^{L_{module}} \int_0^{L_{refl}} E_i \rho \frac{D(\theta, \theta')}{\int_0^{\frac{\pi}{2}} D(\theta, \theta') d\theta} cos(\theta') \frac{cos(\beta)}{r} dxdy \quad (5)$$

Where Qo is the radiant intensity (W) on the surface of the module, ρ is the spectacularly constant surface reflectivity, (θ') is constant for a given time step, and θ, β, and r are a function of the linear distances along reflector and module, x and y:

$$\theta = \pi - sin^{-1}\left[\frac{vsin(\beta+\gamma)}{x^2+y^2-2xycos(\beta+\gamma)})\right] \quad (6)$$

$$\beta = \theta + 180 - (\gamma + \omega) \quad (7)$$

$$r = \sqrt{(x^2+y^2-2xy\cos(\gamma+\omega)} \quad (8)$$

And D(θ,θ') is given by the Beckmann distribution [26].

$$D(\theta, \theta') = \frac{1}{m^2 cos^4(\alpha)} exp^{\frac{cos^2(\alpha)-1}{m^2 cos^2(\alpha)}} \quad (9)$$

Where m is a physical parameter that represents the rms slope of surface roughness on the reflecting surface and generally $m \in [0\ 0.5]$. α is the angle from the surface normal of the vector bisecting θ and θ'.

The BDRF of the two surfaces used in this study were measured using the techniques from section II-B. The theoretical approximations for the BDRF using equation 9 were also calculated for values of m=0.2 for the specular reflector and m=0.8 for the semi-diffuse reflector, and the comparison of the experimental and theoretical values is shown in Fig 4

The diffuse contribution was evaluated using the diffuse view factor between the reflector and PV module, as described by [30], and shown in Equation 10:

$$ViewFactor = \frac{R+1-(R^2+1-2*R*cos(\alpha))^{\frac{1}{2}}}{2} \quad (10)$$

Where R is the ratio of module length to reflector length, and α is the angle between the two surfaces.

C. Model Implementation

This BDRF model was then run iteratively for the full measured dataset of incoming irradiance and zenith angles, and the dual integration was run at each step. The amount of irradiation that directly impacts the module was evaluated using the Perez irradiation translation model [31]. Once the total in-plane irradiation on the face of the module was evaluated, the predicted module output was calculated using the methodologies outlined in [32] using coefficients derived from the control module. Note that only I_{sc} was collected from the modules, and therefore the validation of the model was performed using I_{sc} rather than power. I_{sc} is an excellent predictor of effective irradaince on the plane of the array, and is therefore well suited for validating the model. However, when comparing the annual outputs from the modules, the collected I_{sc} is utilized to calculate effective irradiance, E_e in the Sandia Array Performance Model [33], and used with the collected cell temperature to estimate the power production from each module.

D. Thermal model

In order to predict the temperature of modules under low concentration, the Sandia cell temperature model [33] was modified to better resemble the physical system. Thus, the thermal model utilized for this study is :

$$T_{Cell} = E_B * C_0 + E_D * C_1 + exp(WS * C_2) + T_a \quad (11)$$

Coefficients were derived using a least-squares optimization and were found to be C_0=0.046,C_1=0.106,C_2=-0.116. These coefficients give a Normalized RMSE of 8% and a MBE of -1%, which is an acceptable fit for this application.

Interestingly, the measured data showed temperature spkies for short periods during the day, where the cell to which the thermocouple was attached could reach temperatures approaching $100°C$ for a short period of time, as seen in figure 5. One possible explanation is that these spikes are due to inconsistent illumination from the reflector, however the reflector is relatively uniform, and another possibility is that these temperature spikes are due to the normal "patchwork" appearance of cell temperatures for a short-circuited module, as shown in Fig 6.

E. Model Results

From Fig 7 it can be seen that the new model predictions are in reasonable accord with the experimental data. The prismatic glass module was fit with an NRMSE of 5% and an MBE of 2%, and the flat glass module was fit with an RMSE of 4% and an MBE of 0.2%. Previous work had utilized a geometric optical model, which showed a mid-day dip in intensity. This was caused when the beam of reflected irradiation was projected above the top of the PV module, and thus the proportion of irradiation on the PV module was reduced. This effect is still present in the new BDRF, however

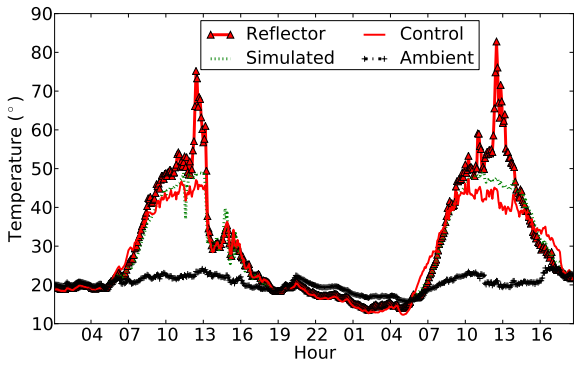

Fig. 5: Thermal variations for May 29 and May 30, showing the thermal spike effect, and the fit of the proposed thermal model.

Fig. 6: *Top:*Two Infrared photographs of a module backsheet, with reflector augmentation taken 1 minute apart. A moving patchwork of hotspot cells is apparent.*Bottom:* veiw of multiple short-circuited modules. Only the modules highlighted with the white circle have reflector augmentation.

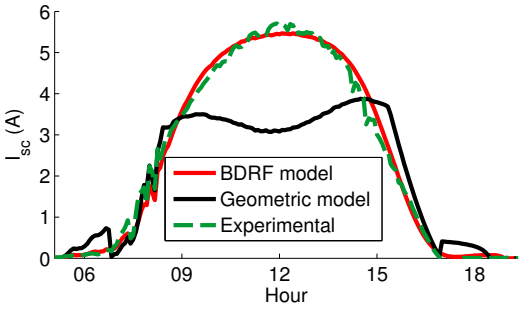

Fig. 7: Comparison of modelled and experimental inrease in I_{sc} output due to reflector. The BDRF utilized ρ=0.9, m=0.09, and the geometric inputs (reflector and module lengths and angles) from the test system.

it is represented more realistically, because the off-specular components of the reflected irradiance are still incident on the module surface. Thus, there is room for improvement of the experimental system, as the original test system was designed and optimized using the geometric optical model, and therefore it can be predicted that a re-optimization of the reflector system will further increase system performance.

It can also be seen that the accuracy of this model can be further improved. Because of the assumption that all incident irradiation will be projected onto a 2D plane, the effects of non-specular scattering along a long semi-diffuse reflector are not fully accounted for. As can be seen in Fig 8, there is an additional increase in energy collected by the flat glass module in the morning, as the module is exposed to diffuse reflections from along the entire length of the reflector. Because the module is positioned slightly to the west of the reflector, in the afternoon this effect is not as pronounced as there is not as much of a length of reflector to the west of the module, and production falls more closely into line with the two dimensional assumption. Therefore, the proposed model could be expanded to include an additional term that accounts for this reflector brightening effect.

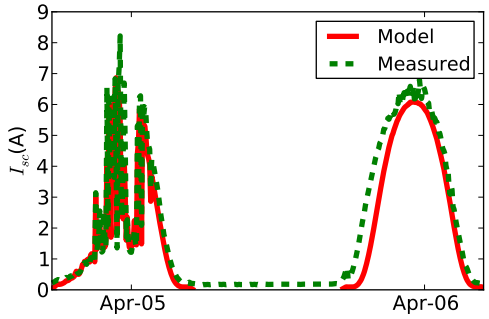

Fig. 8: Two days of production demonstrating the morning reflector brightening as seen by the flat glass module.

IV. Experimental Results

Fig 9 shows the relative increase in calculated P_{mp} between reflector and control modules, averaged weekly over a year. On average, the use of a non-tracking planar reflector can increase system performance (as characterized by $\int P_{mp}$) by **45%** for a traditional flat glass module and by **35%** for a prismatic glass module. There is a large difference in the performance of the two modules, however, based on an analysis of the performance data of the prismatic glass modules, it has been seen that there is a large variance in the power tolerances of these modules. Therefore, it is possible that the prismatic glass module is starting from a lower baseline than its matched control module, which would explain its poorer relative performance.

The effects of the reflector are also characterized in Fig 10, which shows the dependence of output ratio on solar zenith angle over the year for non-cloudy days for all modules.

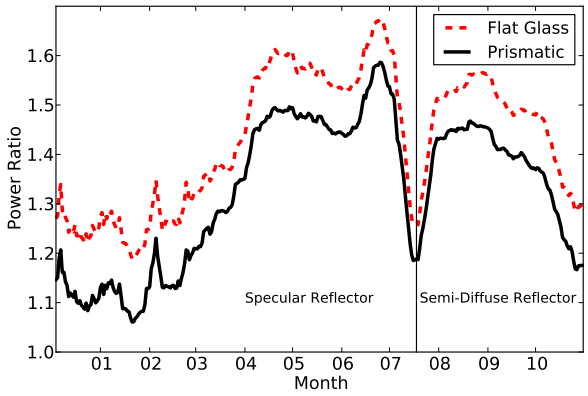

Fig. 9: Timeseries of daily power boost due to reflectors as compared to control modules, averaged over a one week period. The decrease in performance in July represents the time when the reflectors were reduced to horizontal in order to change the reflective material.

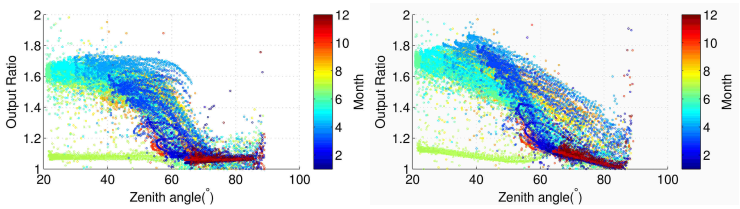

(a) Flat Glass (b) Prismatic Glass

Fig. 10: Clear day output ratios as a function of zenith angle for one year of data

Finally, Fig 11 displays a probability density function for module temperature during the day. It can be seen that for the majority of operation, the module operates below or near to NOCT, however there are some occasions where the cell temperature rises above $90°C$ which could cause issues with some commercial modules.

V. Future Work

This work can be expanded by applying the developed model to a full system optimization in order to determine the optimal arrangement of module and reflector for a given location. This optimization can also take into account practical

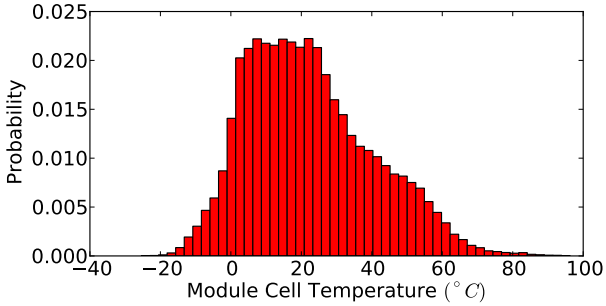

Fig. 11: A probability distribution plot of cell temperatures for the modules under concentration.

system integration issues, in order to make sure that the majority of the energy would be produced during periods where the inverter is not already at capacity. Thus, the sytem could be optimized to maximize total energy yeild, or could be optimized to produce more energy in the mornings and evenings in order to provide passive load balancing.

VI. Conclusions

From this analysis it can be seen that the use of non-tracking planar concentrators are a low cost method of increasing the performance of traditional PV systems. Over a year of outdoors testing, the system has been shown to improve energy yield (as characterized by $\int P_{mp}$) by **45%** for a traditional flat glass module and by **35%** for a prismatic glass module. A new BDRF-based radiance model was introduced, which improved the modelling accuracy and allows for the analysis of non-specular reflectors in low-concentration PV. In the future this new modelling methodology can be used to optimize the reflector topology and identify the potential for increased energy harvest for existing PV systems.

Acknowledgements

The authors would like to acknowledge the work of H. McLaren, J. Fairborn, Q. Bentley, D. Carter and A. Babasola and the support of the Sustainable Energy Applied Research Centre at St. Lawrence College, and to the forward-looking industry partners of this project who made it possible. This project was supported by the Natural Sciences and Engineering Research Council of Canada and a Social Sciences and Humanities Research Council of Canada grant.

References

[1] J. M. Pearce, "Photovoltaics – a path to sustainable futures," *Futures*, vol. 34, no. 7, pp. 663–674, Sep. 2002.

[2] K. Branker, M. Pathak, and J. Pearce, "A review of solar photovoltaic levelized cost of electricity," *Renewable and Sustainable Energy Reviews*, vol. 15, no. 9, pp. 4470–4482, Dec. 2011.

[3] I. R. Cole and R. Gottschalg, "Modelling the efficiency of terrestrial photovoltaic systems," in *Proceedings, Photovoltaic Science, Applications and Technology (PVSAT-6)*, University of Southampton, UK, 2010, this is a conference paper.

[4] M. RNNELID and B. KARLSSON, "The use of corugated booster reflectors for solar collector fields," *Solar Energy*, vol. 65, no. 6, pp. 343–351, Apr. 1999.

[5] H. Chiam, "Stationary reflector-augmented flat-plate collectors," *Solar Energy*, vol. 29, no. 1, pp. 65–69, 1982.

[6] D. Grimmer, K. Zinn, K. Herr, and B. Wood, "Augmented solar energy collection using different types of planar reflective surfaces; theoretical calculations and experimental results," *Solar Energy*, vol. 21, no. 6, pp. 497–501, 1978.

[7] D. McDaniels, D. Lowndes, H. Mathew, J. Reynolds, and R. Gray, "Enhanced solar energy collection using reflector-solar thermal collector combinations," *Solar Energy*, vol. 17, no. 5, pp. 277–283, Nov. 1975.

[8] S. C. Seitel, "Collector performance enhancement with flat reflectors," *Solar Energy*, vol. 17, no. 5, pp. 291–295, Nov. 1975.

[9] L. T. Kosti and Z. T. Pavlovi, "Optimal position of flat plate reflectors of solar thermal collector," *Energy and Buildings*, vol. 45, pp. 161–168, Feb. 2012.

[10] M. D. J. Pucar and A. R. Despic, "The enhancement of energy gain of solar collectors and photovoltaic panels by the reflection of solar beams," *Energy*, vol. 27, no. 3, pp. 205–223, Mar. 2002.

[11] B. Perers, B. Karlsson, and M. Bergkvist, "Intensity distribution in the collector plane from structured booster reflectors with rolling grooves and corrugations," *Solar Energy*, vol. 53, no. 2, pp. 215–226, Aug. 1994.

[12] M. Hall, A. Roos, and B. Karlsson, "Reflector materials for two-dimensional low-concentrating photovoltaic systems: the effect of specular versus diffuse reflectance on the module efficiency," *Progress in Photovoltaics: Research and Applications*, vol. 13, no. 3, p. 217233, 2005.

[13] S. L. Grassie and N. R. Sheridan, "The use of planar reflectors for increasing the energy yield of flat-plate collectors," *Solar Energy*, vol. 19, no. 6, pp. 663–668, 1977.

[14] H. Tanaka, "Solar thermal collector augmented by flat plate booster reflector: Optimum inclination of collector and reflector," *Applied Energy*, vol. 88, no. 4, pp. 1395–1404, Apr. 2011.

[15] H. M. S. Hussein, G. E. Ahmad, and M. A. Mohamad, "Optimization of operational and design parameters of plane reflector-tilted flat plate solar collector systems," *Energy*, vol. 25, no. 6, pp. 529–542, Jun. 2000.

[16] J. W. Bollentin and R. D. Wilk, "Modeling the solar irradiation on flat plate collectors augmented with planar reflectors," *Solar Energy*, vol. 55, no. 5, pp. 343–354, Nov. 1995.

[17] B. Perers and B. Karlsson, "External reflectors for large solar collector arrays, simulation model and experimental results," *Solar Energy*, vol. 51, no. 5, pp. 327–337, 1993.

[18] T. Matsushima, T. Setaka, and S. Muroyama, "Concentrating solar module with horizontal reflectors," *Solar Energy Materials and Solar Cells*, vol. 75, no. 34, pp. 603–612, Feb. 2003.

[19] Rob W. Andrews, Nabeil Alazzam, and Joshua M. Pearce, "Model of loss mechanisms for low optical concentratioon on solar photovoltaic arrays with planar reflectors," in *40th American Solar Energy Society National Solar Conference Proceedings*, Rayleigh NC, 2011, pp. 446–453.

[20] J. Laird, "Facility puts solar products to test," *Renewable Energy Focus*, vol. 12, no. 5, pp. 20–22, Sep. 2011.

[21] J. M. Pearce, A. Babasola, and R. Andrews, "Open solar photovoltaic systems optimization," *Proceedings of the 16th Annual National Collegiate Inventors and Innovators Alliance Conference, Open 2012*, 2012.

[22] C. E. Kennedy and K. Terwilliger, "Optical durability of candidate solar reflectors," *Journal of Solar Energy Engineering*, vol. 127, no. 2, pp. 262–269, Apr. 2005.

[23] R. L. Cook and K. E. Torrance, "A reflectance model for computer graphics," *ACM Trans. Graph.*, vol. 1, no. 1, p. 724, Jan. 1982.

[24] Christophe Schlick, "An inexpensive BRDF model for physcially-based rendering," *Computer Graphics Forum*, vol. 13, no. 3, pp. 233–246, 1994.

[25] M Hall, A Roos, and Bjrn Karlsson, "Reflector materials for two-dimensional low-concentrating photovoltaic systems: the effect of specular versus diffuse reflectance efficiency on the module," *Progress in Photovoltaics: Research and Applications*, vol. 13, no. 3, pp. 217 – 233, 2005.

[26] P. Beckmann and A. Spizzichino, "The scattering of electromagnetic waves from rough surfaces," *Norwood, MA, Artech House, Inc., 1987, 511 p.*, vol. -1, 1987.

[27] K. E. TORRANCE and E. M. SPARROW, "Theory for off-specular reflection from roughened surfaces," *Journal of the Optical Society of America*, vol. 57, no. 9, pp. 1105–1112, Sep. 1967.

[28] X. D. He, K. E. Torrance, F. X. Sillion, and D. P. Greenberg, "A comprehensive physical model for light reflection," *SIGGRAPH Comput. Graph.*, vol. 25, no. 4, p. 175186, Jul. 1991.

[29] K. J. Dana, B. van Ginneken, S. K. Nayar, and J. J. Koenderink, "Reflectance and texture of real-world surfaces," *ACM Trans. Graph.*, vol. 18, no. 1, p. 134, Jan. 1999.

[30] P. Schrder and P. Hanrahan, "On the form factor between two polygons," in *Proceedings of the 20th annual conference on Computer graphics and interactive techniques*, ser. SIGGRAPH '93. New York, NY, USA: ACM, 1993, p. 163164.

[31] R. Perez, P. Ineichen, R. Seals, J. Michalsky, and R. Stewart, "Modeling daylight availability and irradiance components from direct and global irradiance," *Solar Energy*, vol. 44, no. 5, pp. 271–289, 1990.

[32] R. W. Andrews, A. Pollard, and J. M. Pearce, "Improved parametric empirical determination of module short circuit current for modelling and optimization of solar photovoltaic systems," *Solar Energy*, vol. 86, no. 9, pp. 2240–2254, Sep. 2012.

[33] D. L. King, W. E. Boyson, and J. A. Kratochvil, "Photovoltaic array performance model," *Sandia*, vol. SAND2004-3535, Aug. 2004.